Bulgarian Journal of Physics vol. **47** (2021) 70–77

Compact Scintillator Detector for Sub-MeV and MeV Gamma-Ray Astronomy

Zh. Toneva, **S. Ivanov**, **S. Lalkovski**

Faculty of Physics, University of Sofia "St. Kl. Ohridski",
5 James Bourchier Boulevard, BG-1164 Sofia, Bulgaria

Received *7 December 2020*

Abstract. Gamma-ray energy and direction measurement have played an essential role in many fields such as astrophysics, medical physics and homeland security. With new technological developments, the available methods can achieve better scientific output. For example, using a new concept of an instrument with position sensitive-scintillation detector, based on monolithic scintillator and multi-pixel photo-sensor, one can improve the current knowledge in gamma-ray imaging. This study covers a research of instrument which is able to perform spectroscopy and imaging while maintaining small dimensions compared to modern solutions. We report here results on our conceptual design of a compact position-sensitive scintillator detector for sub-MeV and MeV gamma-ray energy range. Simulations via Geant4 toolkit data for efficiency and single Compton event distributions are presented and discussed.

KEY WORDS: scintillation detectors, gamma-ray astronomy

1 Introduction

Gamma-ray astronomy in the sub-MeV and MeV energy range, is one of the most challenging fields due to the technical and detection limits of the available techniques one is facing in space. This energy range, however, is still not well explored despite the numerous objects of high scientific interest. The fast developments in new technologies for detection of sub-MeV and MeV energies are of great support for gamma-ray astronomy. The need for novel gamma-ray detectors for low and medium energy range has never been greater. In the past decades, there was only one operating telescope observing the sky in the above-mentioned energy range - INTEGRAL [1]. The INTEGRAL mission has several subsystems among which the SPI and the IBIS. The SPI module is used for spectroscopy and its detection principle is based on cooled Ge detectors, a coded mask and active shielding. The IBIS module is an imager with two detector layers, i.e. CdTe and CsI arrays, equipped as well with a coded mask. The technologies used for SPI and IBIS date back to the 1990s, which makes them

large, heavy and hard to maintain compared to modern standards. The quickly approaching end of the INTEGRAL mission makes the future of observations in sub-MeV and MeV energy range unclear. Thus, several large-scale missions are being considered to replace INTEGRAL, namely ASTROGAM [2] in Europe, COMPAIR [3] and AMEGO [4] in the US. The latter are still at the approval stage. If approved, these complex missions will be ready for use only as early as the 2030s.

The time gap between the present and future missions could be bridged by easily assembled, small-scale telescope. Its development should be suitable to the existing CubeSat technology [5] making it also inexpensive. The CubeSat technology is proven to be a great tool for building missions affordable by national funding agencies, research centres and universities. Based on the future needs of sub-MeV and MeV gamma-ray astronomy and taking advantage of state-of-the-art nano-satellites technologies, the present study is devoted to the development of a novel detector technology that potentially can be used in space-borne telescopes, for both imaging and spectroscopy.

2 Approach and Materials

2.1 Concept of the compact space-borne nano-telescopes

Our conceptual design for a new compact space-borne telescope in sub-MeV and MeV region was inspired by the Compton camera telescope idea used in COMPTEL [8], on board of the Compton Gamma Ray Observatory. Based on that we research compact position-sensitive detector that can be used in the composition of Compton camera placed in CubeSat modules. As shown in Figure 1,

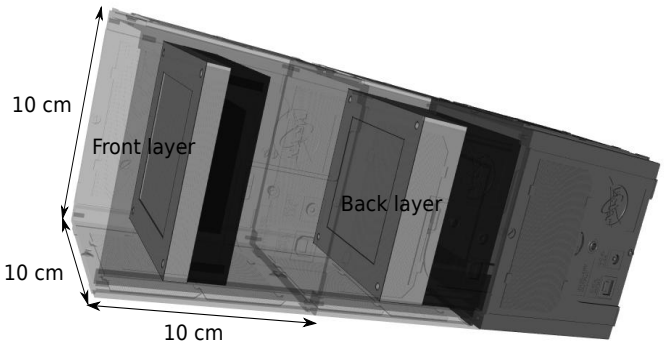

Figure 1. Prototype of a nanosatellite with Compton camera designed in our group and placed inside 3 units CubeSat modules, designed by NASA [6]. Each detector consists of monolithic scintillation crystal coupled to a multi-pixel photomultiplier [7].

the gamma-ray telescope plan to have two detector layers. Each layer consists of a monolithic scintillator coupled to a position-sensitive light sensor. The purpose of the front layer (scatterer) is to scatter incident gamma photons and will be placed close to the aperture of the telescope. The scatterer has to have optimal geometry in respect of detecting single Compton scattering process. The second layer (absorber) will be optimized to absorb the scattered from the first layer gamma rays. The two layers planes must be placed in such distance of each other so to achieve optimal spatial resolution. To reproduce the position of incidence precisely, the two detector layers have to have good position resolutions. Fast gamma-gamma coincidence circuits will be used to eliminate background events.

Considering CubeSat technology and geometry, a few constraints must be faced. The telescope has to have dimensions, weight, power consumption and geometry suitable for nano-satellite. The present approach, as much inspired by COMPTEL, relies on the most recent developments in scintillator and photomultiplier technologies. As such, we aim to achieve a better position- and energy- resolutions when compared to COMPTEL but reducing the size of the mission.

2.2 Requirement of the position-sensitive scintillation detector

The researched detector aims to be used to identify space-borne sources within 100 keV up to 2 MeV. Given that a single detector is expected to provide spectroscopic information and generate images of astronomical objects, its position resolution should be better than 5 mm, which is a prerequisite for the generation of sharp images. An energy resolution of 5% at 662 keV is required, for identification and disentanglement of different radiation sources. To secure good background subtraction via fast gamma-gamma circuit, a time resolution of the order of 150 ps is needed. For reducing the observation time, high efficiency is also required.

2.3 Scintillators

In this study, scintillators of the family of the lanthanum-halide have been used, in particular $CeBr_3$ and $LaBr_3$:Ce. Those materials have high light yield, good energy and time resolution. Comparative characteristics of $CeBr_3$ and $LaBr_3$:Ce, are presented in Table 1. The lower light yield of $CeBr_3$ [9], when compared to $LaBr_3$:Ce [10], results in poorer energy resolution. However, $CeBr_3$ material has low intrinsic activity when compared to the $LaBr_3$:Ce. This would result in 25 times shorter observation time if $CeBr_3$ is used instead of $LaBr_3$:Ce detectors of the same size and geometry [9]. Calculation for the angular distribution of the scattered gamma rays in $CeBr_3$ and $LaBr_3$:Ce was made using Klein-Nishina formula for the differential cross section. The distribution is shown in Figure 2 and illustrate the strong tendency for forward scattering at high gamma-ray energy and the advantage of higher Z scintillators as $CeBr_3$. Because of the linear Z

Table 1. Comparison between $CeBr_3$ and $LaBr_3$:Ce scintillator material. Energy resolution FWHM is taken for $E_\gamma = 662$ keV [9], [11], time resolutions in FWHM for $CeBr_3$ [12] and $LaBr_3$:Ce [13] is obtained for $E_\gamma = 511$ keV, and position resolution at $E_\gamma = 356$ keV [14]. [7]

	Energy resolution [%]	**Time resolution [ps]**	**Position resolution [mm]**	**Light yield ph/MeV]**	**Peak emission [mm]**
$CeBr_3$	4	210	5.4	45 000	380
$LaBr_3$:Ce	3	154	8.0	63 000	370

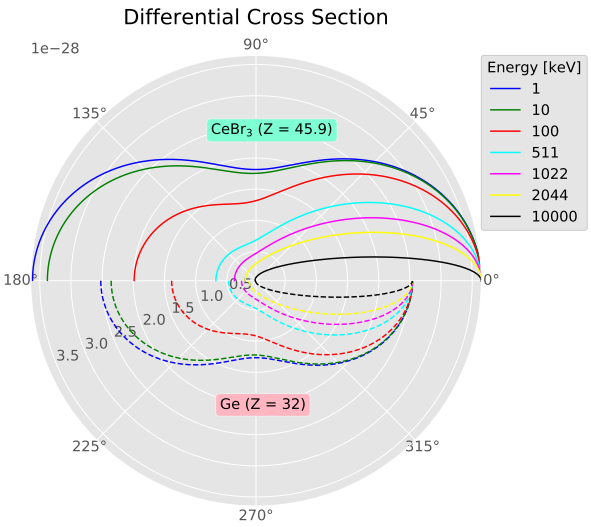

Figure 2. A polar plot of the number of Compton scattered photons (incident from the left) for $CeBr_3$ and $LaBr_3$:Ce. Colour curves shows different energies.

dependency, $CeBr_3$ scatters 1.43 times more than Ge detectors in all directions. One could also consider BGO scintillators as they have higher Z compared to the $CeBr_3$, however, their energy resolution is worse making them unsuitable for the above mentioned concept of nano-satellite.

2.4 Geant4 simulations

Our studies were carried out using the Geant4 simulation framework, which is an object-oriented C++ Monte Carlo (MC) toolkit that allows the construction of customized geometrical setups, the interaction between particles and the tracking of particles in the medium [15]. The toolkit has a broad range of electromagnetic packages. Customized physics package including main observed processes has been implemented. User-defined geometry is used for $CeBr_3$ and $LaBr_3$:Ce

scintillators. Two configuration codes were developed. The first code is used to study the distribution of the single Compton interaction events that occur within scintillators with different thickness and for range of energies. The second is to estimate the efficiency of the different scintillators for energies in the range of about 0.1 to 2 MeV. In both simulations, the gamma-ray source and the scintillators with the optical window were included. We have utilized a point-like source with predefined gamma-ray beam. In both simulations, detector geometry was imported into Geant4 through GDML [16].

3 Results and Discussion

Measurement previously done by our group for $CeBr_3$ scintillators shows good position-resolution and hardly sufficient energy resolution. Results and analysis are presented in [7, 17]. Here we would like to present further characterizations for $CeBr_3$ with three different thicknesses while comparing their results with those for $LaBr_3$:Ce. Geant4 simulations for $CeBr_3$ with tree different thicknesses and one for $LaBr_3$:Ce were made. We simulated 10 mm and 25 mm thick $CeBr_3$ scintillator and 1'$\times$1' $LaBr_3$:Ce, readily available detectors at our laboratory. Furthermore, the varieties of geometries of a 40 mm, 100 mm and 200 mm $CeBr_3$ were investigated for the efficiency. For single Compton events following scintillator thicknesses were investigated - form 1 mm up to 15 mm with step of 1 mm, from 15 mm up to 50 mm with step of 5 mm, and form 50 mm up to 220 mm with step of 10 mm.

One of our simulation study the single Compton, and only, interaction toward beam direction. In Figure 3 one can see the single Compton scattering as per

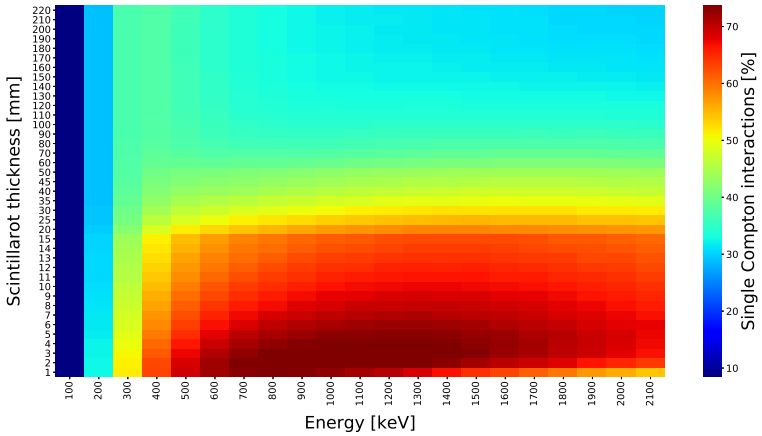

Figure 3. First Compton interaction events for different gamma rays energies and $CeBr_3$ scintillation thicknesses.

cent of the all occurred Compton interactions inside the detector volume. The maximum of single Compton interactions is observed for scintillators with thicknesses 2–3 mm for energies between 600–1600 keV. For scintillators with approximately 10 mm thickness the number of single Compton scatterers is similar for broader energy range, which makes it good candidate for the first layer of the nano-satellite. Furthermore, the 10 mm thickness fits well within the CubeSat geometry specifications, which will keep the design rather compact.

The second simulation allows us to investigate how the detection efficiency curves evolve with initial gamma energy, see Figure 4. We observe different behaviour for all thicknesses, while having almost equal high efficiency at lower energies, around 95%, it rapidly changes for higher energy, dropping down to a maximum of 20%. In the case of the absorber, it is necessary to have the most efficient thickness, which our study shows that the 40 mm $CeBr_3$ would be the best candidate.

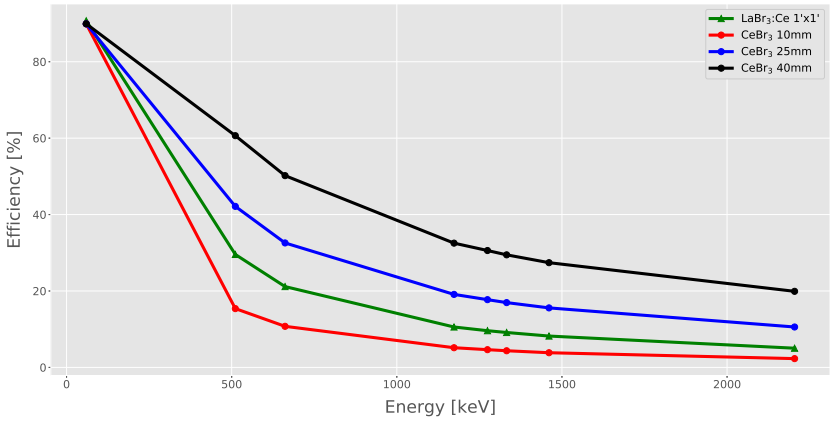

Figure 4. Scintillators efficiency for different gamma rays energies.

4 Conclusions

We have shown in our simulation close to 75% of all scattered gamma-ray photons have a single interaction for $CeBr_3$ with thickness close to 10 mm. Our investigation shows that scatterer and absorber with a thickness of 10 and 40 mm, respectively, will meet the space constrains from CubeSat and will provide with good detector performance in the sub-MeV and MeV energy range.

Acknowledgements

This work is supported by the Bulgarian National Science Fund under contract number DN18/17.

References

[1] ESA INTEGRAL. https://sci.esa.int/web/integral.
[2] A. De Angelis et al. (2018) Science with e-ASTROGAM: A space mission for MeV–GeV gamma-ray astrophysics. *JHEAp* **19** 2018/08/01 1-106 DOI: https://doi.org/10.1016/j.jheap.2018.07.001.
[3] A. Moiseev et al. (2015) Compton-Pair Production Space Telescope (ComPair) for MeV Gamma-ray Astronomy. arXiv:1508.07349 [astro-ph.IM].
[4] Sean Griffin (2019) Subsystem Development for the All-Sky Medium Energy Gamma-ray Observatory (AMEGO) prototype. Presented at *36th International Cosmic Ray Conference* (ICRC2019).
[5] CubeSat CubeSat standard https://www.cubesat.org/.
[6] NASA 3D Resources, CubeSat https://nasa3d.arc.nasa.gov/detail/cubesat.
[7] Zh. Toneva et al. (2020) Study of a small scale position-sensitive scintillator detector for γ-ray spectroscopy. *JINST* **15** 1 C01013–C01013 DOI: https://doi.org/10.1088/1748-0221/15/01/C01013 .
[8] V. Schonfelder (1993) Instrument description and performance of the Imaging Gamma-Ray Telescope COMPTEL aboard the Compton Gamma-Ray Observatory *ApJS* **86** 6 657-692 DOI: 10.1086/191794 .
[9] F.G.A. Quarati et al. (2013) Scintillation and detection characteristics of high-sensitivity $CeBr_3$ gamma-ray spectrometers. *Nucl. Instrum. Methods Phys. Res., Sect. A* **729** 596-604 DOI: https://doi.org/10.1016/j.nima.2013.08.005.
[10] S. Lo Meo et al. (2009) Optical physics of scintillation imagers by GEANT4 simulations. *Nucl. Instrum. Methods Phys. Res., Sect. A* **607** 1 259-260 DOI: https://doi.org/10.1016/j.nima.2009.03.168.
[11] A. Gostojic et. al. (2016) Characterization of $LaBr_3$:Ce and $CeBr_3$ calorimeter modules for 3D imaging in gamma-ray astronomy. *Nucl. Instrum. Methods Phys. Res., Sect. A* **832** 1 October 2016 24-42 DOI: https://doi.org/10.1016/j.nima.2016.06.044.
[12] L.M. Fraile et al. (2013) Fast timing study of a $CeBr_3$ crystal: Time resolution below 120 ps at ^{60}Co energies. *Nucl. Instrum. Methods Phys. Res., Sect. A* **701** 11 February 2013 235-242 DOI: https://doi.org/10.1016/j.nima.2012.11.009.
[13] M. Moszynski et al. (2006) New Photonis XP20D0 photomultiplier for fast timing in nuclear medicine. *Nucl. Instrum. Methods Phys. Res., Sect. A* **567** 1 31-35 DOI: https://doi.org/10.1016/j.nima.2006.05.054.
[14] A. Ulyanov et al. (2017) Localisation of gamma-ray interaction points in thick monolithic $CeBr_3$ and $LaBr_3$:Ce scintillators. *Nucl. Instrum. Methods Phys. Res., Sect. A* **844** 1 February 2017 81-89 DOI: https://doi.org/10.1016/j.nima.2016.11.025.
[15] S. Agostinelli et al. (2003) Geant4 – a simulation toolkit. *Nucl. Instrum. Methods Phys. Res., Sect. A* **506** 3 250-303 DOI: https://doi.org/10.1016/S0168-9002(03)01368-8.

[16] GEANT4 collaboration GDML USER′S GUIDE. http://lcgapp.cern.ch/project/simu/framework/GDML/doc/GDMLmanual.pdf.

[17] Zh. Toneva et al. (2019) Research and Development of a Position-Sensitive Scintillator Detector for γ- and X -Ray Imaging and Spectroscopy. In: García-Ramos, J.-E., Andrés, M.V., Valera, J.A.L., Moro, A.M., Pérez-Bernal, F. (eds.) "Basic Concepts in Nuclear Physics: Theory, Experiments and Application". *Springer Proc. Phys.* vol. **225**, Springer International Publishing, pp. 247-249 DOI: https://doi.org/10.1007/978-3-030-22204-8_l40.